Journal of Physics and Chemistry of Solids 169 (2022) 110836

Contents lists available at ScienceDirect

Journal of Physics and Chemistry of Solids

journal homepage: www.elsevier.com/locate/jpcs

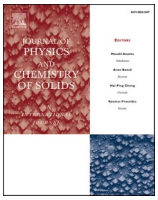

Novel gallium-based voltammetric sensor for sensitive detection of cysteine

Kadir Selçuk [a], Aykut Çağlar [a,c], Nahit Aktas [a,b,*], Hilal Kivrak [c,d]

[a] Van Yuzuncu Yil University, Faculty of Engineering, Department of Chemical Engineering, Van, 65000, Turkey
[b] Kyrgyz-Turk Manas University, Faculty of Engineering, Department of Chemical Engineering, Bishkek, Kyrgyzstan
[c] Eskisehir Osmangazi University, Faculty of Engineering and Architectural Sciences, Department of Chemical Engineering, Eskişehir, 26040, Turkey
[d] Translational Medicine Research and Clinical Center, Eskişehir Osmangazi University, 26040 Eskişehir, Turkey

ARTICLE INFO

Keywords:
Gallium
Carbon nanotubes
Chemisorption
Cysteine
Sensor

ABSTRACT

Carbon nanotube-supported gallium (Ga/CNT) was synthesized and characterized with energy dispersive X-ray-scanning electron microscopy, temperature-programmed reduction, temperature-programmed oxidation, and temperature-programmed desorption methods. Characterization results revealed successful preparation of Ga/CNT. Electrochemical measurements were performed by cyclic voltammetry, differential pulse voltammetry, and electrochemical impedance spectroscopy. The Ga/CNT-based cysteine sensor had a linear response within the range of 0–200 μM with current sensitivity of 0.0081 μA/μM (114 μA/mM cm^2), low detection limit of 0.05 μM, and signal-to-noise ratio of 3. Interference studies revealed that (Ga/CNT)@glassy carbon electrode was not affected by interfering species. Thus, Ga/CNT is a promising cysteine sensor.

1. Introduction

Food is all the substances that living things eat and drink in order to survive. In other words, food is the edible parts of animals and plants, such as meat, milk, bread, and fruit. Nutrition is the obtained by eating and drinking both animal and plant foods. In other words, nutrition is the intake of sufficient amounts of nutrients necessary for human growth, development, healthy and productive life in the long term, and assimilation into the body. The important thing in nutrition is adequate and balanced intake of nutrients. Food is broken down into very small pieces after being taken into the body and these are used in the body in different ways. For example, some of the nutrients consumed can be used in providing energy, some in tissue repair, and some in cell proliferation. Basic nutritional building blocks are proteins, lipids, carbohydrates, vitamins, minerals, and water, and proteins are some of the most important. Proteins are large organic compounds formed by chain linking of amino acids. There are 20 types of amino acids most commonly used in the formation of proteins, from humans to viruses. Cysteine is semi-essential and also a proteinogenic amino acid, with formula HO_2CCH (NH_2) CH_2SH. Cysteine is mostly found in foods high in protein. If enough methionine is available, cysteine can mostly be metabolically synthesized in the human body under normal physiological conditions. Therefore, cysteine is an important amino acid in the diagnosis of various diseases such as growth retardation, hair loss, edema formation, lethargy, liver damage, muscle and fat regression, skin lesions, and fatigue. Cysteine is found in medical, biological, food, and industrial products. Therefore, it is important to develop important nanomaterials for the precise detection of cysteine [1–7]. Various methods such as spectrometric chromatographic separation [8–10], colorimetric [11–17], and electrochemical methods [18–25] are used for detecting cysteine. Electrochemical methods have important advantages including simple detection, inexpensive devices, static miniaturization, and acceptable selectivity. For the electrochemical determination of cysteine, the choice of electrode material and the easy determination of cysteine are important factors. Various electrode materials have been used to enhance electrochemical selectivity of carbon-based electrodes for cysteine in the literature in a wide range of electrochemical sensors due to their lower background current, low cost, chemical inertness, and wide potential range [26–33].

Due to the unique properties of carbon nanotubes (CNTs), CNT-modified electrodes and CNT-supported gallium (Ga) catalyst are promising nanocatalysts in electrode materials for the electrochemical determination of cysteine. In this study, the sodium borohydride ($NaBH_4$) reduction method was used primarily to prepare the Ga/CNT nanocatalyst. Temperature-programmed reduction (TPR), temperature-programmed oxidation (TPO), and temperature-programmed desorption (TPD) analyses were used to determine the reduction, oxidation, and desorption properties of the catalyst, respectively. Energy dispersive

* Corresponding author. Van Yuzuncu Yil University, Faculty of Engineering, Department of Chemical Engineering, Van, 65000 Turkey.
E-mail addresses: nahit.aktas@manas.edu.kg, naktas@yyu.edu.tr (N. Aktas).

https://doi.org/10.1016/j.jpcs.2022.110836
Received 14 May 2021; Received in revised form 6 June 2022; Accepted 7 June 2022
Available online 7 June 2022
0022-3697/

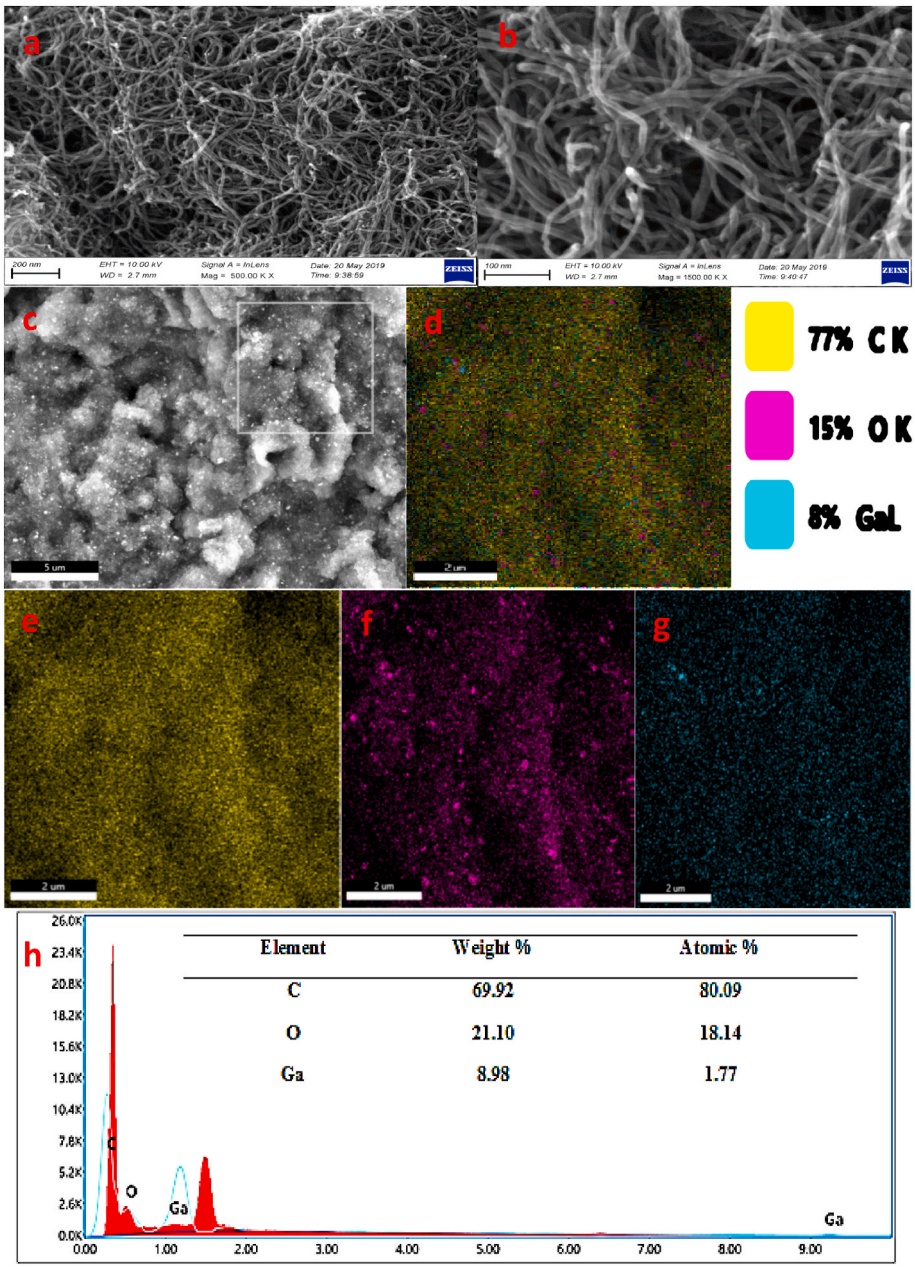

Fig. 1. (a, b, h) EDX-SEM and mapping images [(c, d) mapping and EDX point, (e) C, (f) O, and (g) Ga] of 5% Ga/CNT catalyst.

X-ray-scanning electron microscopy (EDX-SEM) was used to determine surface properties and chemical metal structure. Glassy carbon electrodes (GCEs) were modified with Ga/CNT catalyst. The electrochemical behavior of the (Ga/CNT)@GCE catalyst was examined using cyclic voltammetry (CV), differential pulse voltammetry (DPV), and electrochemical impedance spectroscopy (EIS) methods. The results showed that the (Ga/CNT)@GCE had high sensitivity. Afterward, interference study and real sample analysis were performed using (Ga/CNT)@GCE. Real sample analysis was performed to detect cysteine in a drug sample.

2. Experimental

The L-cysteine (≥99.99%), gallium (III) chloride ($GaCl_3$, ≥99.999%), multi-walled carbon nanotube (MWCNT, 98%), $NaBH_4$ (99%), ascorbic acid (99%), uric acid (≥99%), glucose (≥99.5%), L-tyrosine (≥98%), L-tryptophan (≥98%), and Nafion 117 solution (5%) were obtained from Sigma-Aldrich and used without replacement. The Ga/CNT catalyst containing Ga metal (5% by weight) was synthesized by the $NaBH_4$ reduction method. Materials and preparation methods are given as supplementary information (S1 and S2). These materials were characterized with EDX-SEM, H_2-TPR, O_2-TPO, and NH_3-TPD analyses. The H_2-TPR, O_2-TPO, and NH_3-TPD analyses were completed with a Micromeritics Chemisorb 2750 (gas-adsorption equipment) automated system using ChemiSoft TPx software (supplementary information S3). Firstly, the catalyst ink was prepared. The Ga/CNT catalyst was kept in an ultrasonic bath until homogeneously dispersed in Nafion. Finally, the catalyst ink was transferred to the GCE surface of 3 mm diameter with the help of a micropipette. Cysteine electrooxidation measurements were performed using CV and DPV (supplementary information S4).

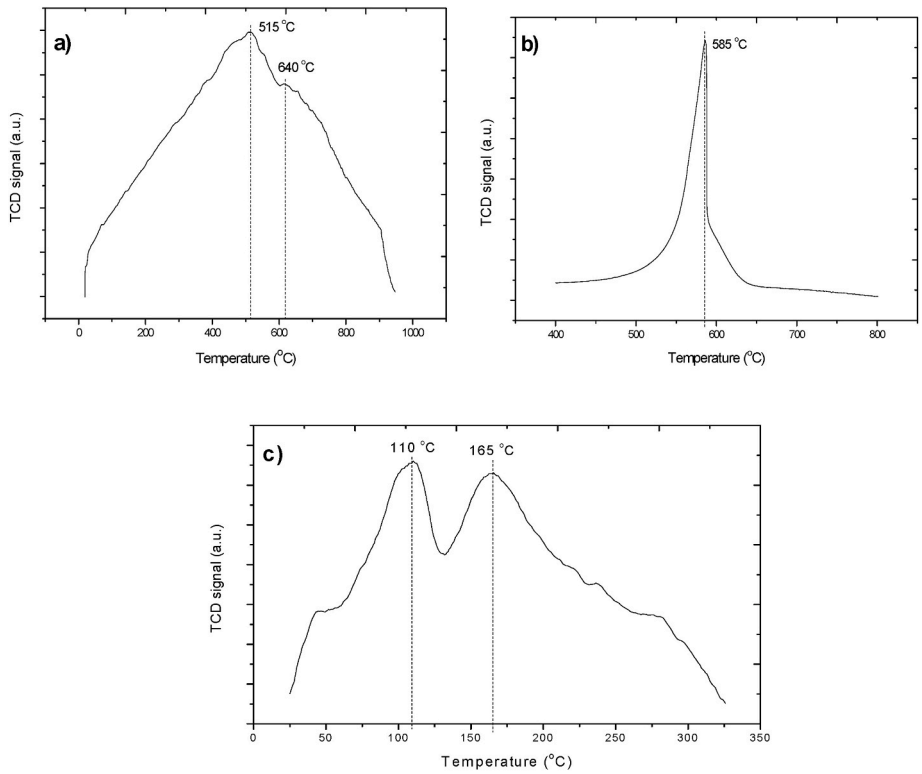

Fig. 2. (a) H_2-TPR, (b) O_2-TPO, and (c) NH_3-TPD profiles of Ga/CNT catalyst.

3. Results and discussion

3.1. Physical characterization

The EDX-SEM and mapping analysis were utilized to investigate the surface morphology of the Ga/CNT catalyst (Fig. 1a–h). There were CNT networks formed (Fig. 1a and b). Furthermore, Ga metal was homogeneously distributed in these networks. The mapping and EDX analysis of the Ga/CNT catalyst were performed on the point depicted in Fig. 1c and d. The analysis results showed that this point contained C, O, and Ga (yellow, pink, and turquoise in Fig. 1e–g, respectively). The % weight and atomic ratios from EDX results of C, O, and Ga elements are shown in Fig. 1h. The EDX-SEM and mapping analysis results showed that the desired structure was obtained.

The H_2-TPR (a), O_2-TPO (b), and NH_3-TPD (c) profiles of Ga/CNT catalyst are depicted in Fig. 2a–c. All analyses were performed at a heating rate of 10 °C/min and a gas flow rate of 50 ml/min. The H_2-TPR analysis was utilized to examine catalyst behavior during reduction with

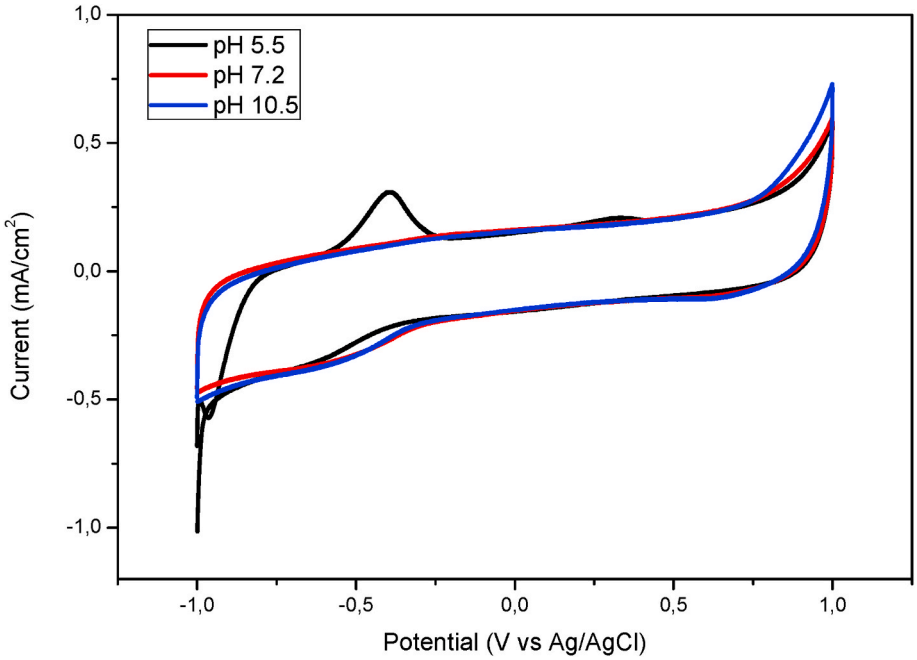

Fig. 3. CV curves of 5% Ga/CNT catalyst at three different pHs (5.5, 7.2, and 10.5) at a scan rate of 100 mV/s in 0.1 M PBS solution.

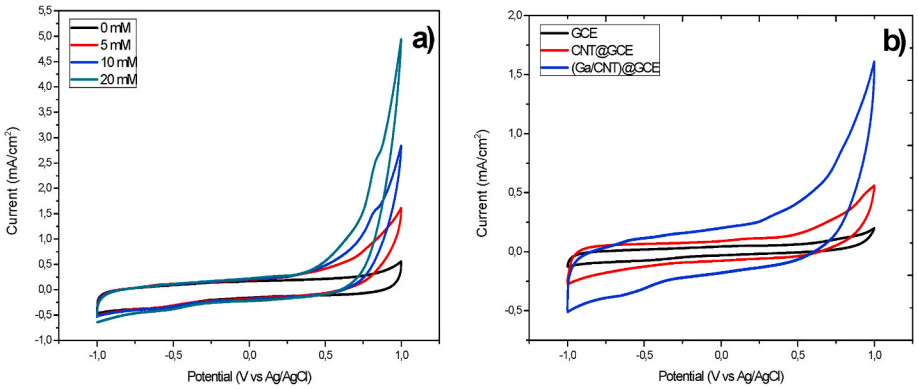

Fig. 4. CV analyses of (a) four different concentrations (0, 5, 10, and 20 mM) of 5% Ga/CNT catalyst and (b) comparison of GCE, CNT@GCE, and (Ga/CNT)@GCE in 5 mM cysteine at a scan rate of 100 mV/s in 0.1 M PBS solution (pH 7.2).

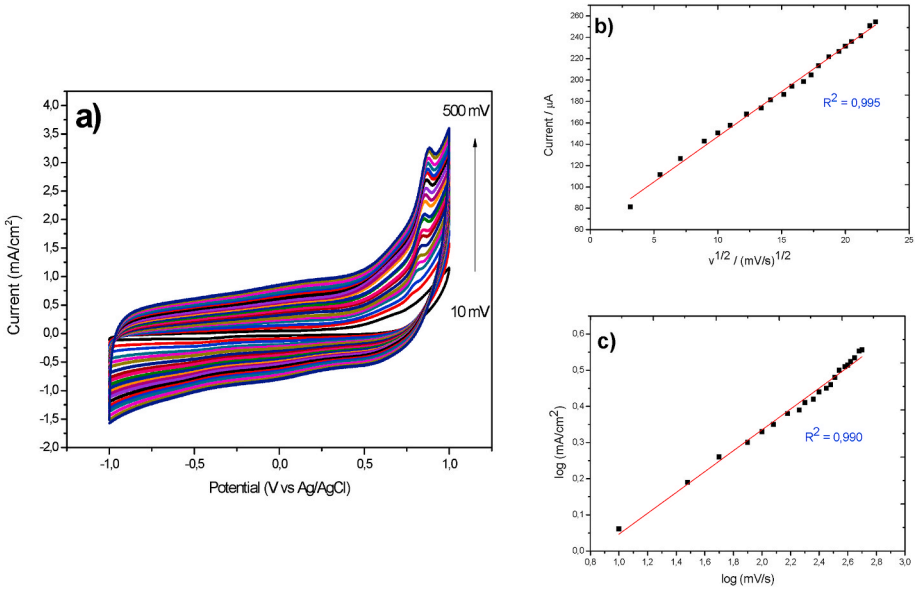

Fig. 5. (a) CV analysis of (Ga/CNT)@GCE at different scan rates (10, 30, 50, 100, 120, 150, 180, 200, 230, 250 300, 320, 350, 380, 400, 420, 450, 480, and 500 mV/s), (b) linear regression of peak currents vs the square root of scan rates, and (c) linear relationship between log current anodic peak vs log scan rates in 0.1 M PBS (pH 7.2) + 5 mM cysteine solution.

H_2. The Ga/CNT catalyst consumed an important amount of H_2 between 25 °C and 800 °C. There were two reduction peaks during H_2-TPR analysis up to 950 °C for the Ga/CNT catalyst, located at 515 °C and 640 °C (Fig. 2a). Beasley et al. [34] reported that the reduction peak for Ga, undoped or without support, was 390 °C. The TPR results for the Ga/CNT catalyst showed the interaction of Ga with CNT, with reduction peaks at high temperatures of 515 °C and 640 °C (Fig. 2a) [34,35]. Fig. 2b shows O_2-TPO analysis of the Ga/CNT catalyst. The TPO analysis is the process of heating a material to a certain temperature by passing an oxidizing gas mixture containing oxygen over it. The Ga/CNT catalyst had a sharp-peaked TPO profile at about 585 °C (Fig. 2b). Feng et al. [36] reported that a MWCNT caused peak oxidation at 640 °C in TPO analysis. Based on this result, the addition of Ga metal to CNT causes a decrease in the oxidation temperature. This is because the surrounding carbon is oxidized before the metal, followed by a loss in metal–carbon contact [37]. The TPD analysis is a characterization process in which an event occurring on the surface of solid material is examined and the temperature of the studied sample is changed by a temperature program. This technique is used to characterize the adsorption sites on the sample. It involves first measuring the desorption rate by adsorption of a known gas on the sample at low temperatures and then heating [38,39]. The NH_3-TPD curve for the Ga/CNT catalyst clearly showed two NH_3 desorption peaks at 110 °C and 165 °C (Fig. 2c), which are attributed to weak and strong acid sites, respectively [40].

3.2. Electrochemical measurements

After adding 1 ml of Nafion solution to 5 mg of the obtained catalyst, this was left in an ultrasonic bath until homogeneously dispersed. This catalyst slurry was used to modify the surface of a GCE for electrochemical detection of cysteine. Firstly, CV analysis of 0.1 M PBS solution was performed at three different pHs of 5.5, 7.2, and 10.5, and the results were close to each other (Fig. 3). Therefore, experiments continued with the solution that was close to neutral (pH 7.2).

The concentration effect on the cysteine electrooxidation activity of Ga/CNT-modified GCE was performed with varying concentrations of cysteine: 0, 5, 10, and 20 mM in PBS (0.1 M at pH 7.2). The activity increases as the cysteine concentration increases [4,41–48]. The Ga/CNT catalyst affected the cysteine detection (Fig. 4a). Furthermore, CV analyses of GCE and CNT@GCE in 5 mM cysteine were performed to demonstrate the effect of Ga metal. The (Ga/CNT)@CNT catalyst had better activity compared to GCE and CNT@GCE (Fig. 4b). According to this result, Ga metal affected cysteine detection.

The sufficiency of the electroactive surface area of (Ga/CNT)@GCE

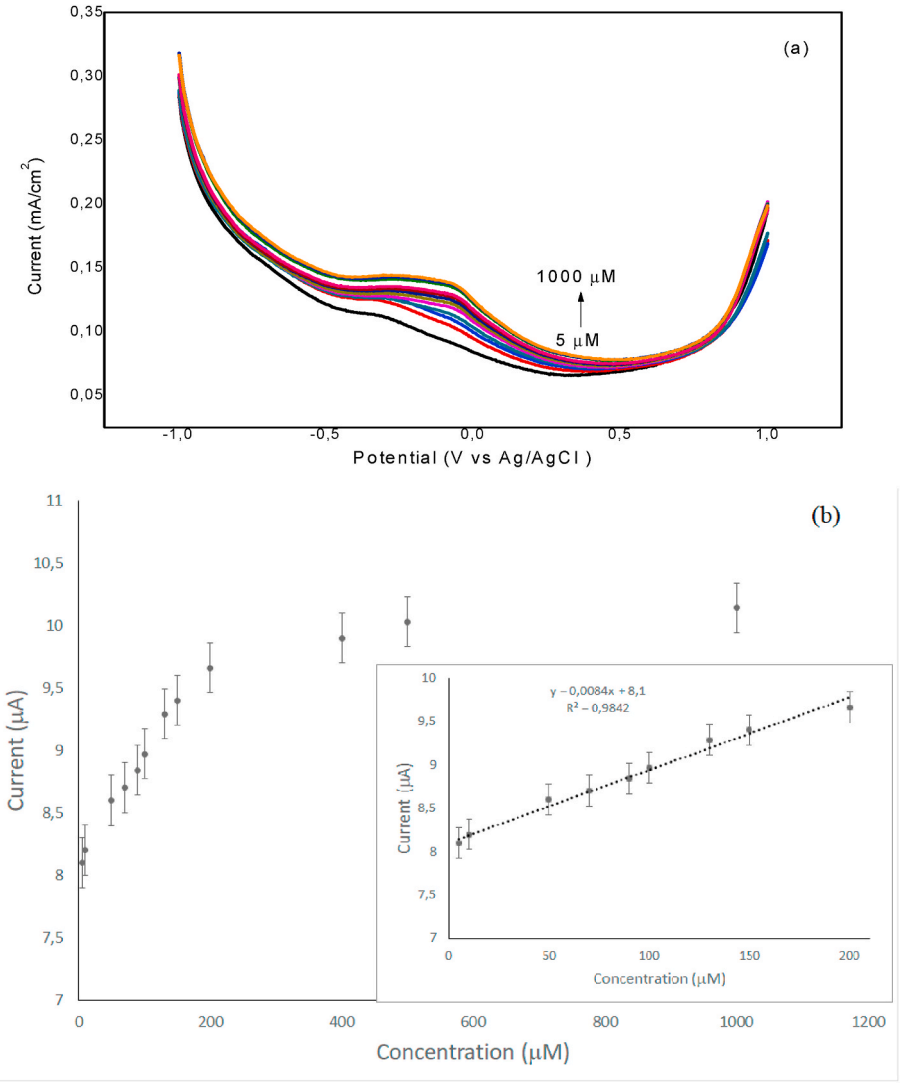

Fig. 6. (a) DPV curves taken at various cysteine concentrations (0–1000 µM), (b) calibration plots at varying cysteine concentrations (0–1000 µM), and insert graph shows the linear range and trendline ($R^2 = 0.9842$).

was appraised using CV measurements for the (Ga/CNT)@GCE in phosphate buffer solution (Fig. 5b), at different scan rates in the range of 10–500 mV/s. The Randles–Sevcik equation follows [49–51]:

$$I_p = 2.69 \times 10^5\ n^{3/2}\ A_{eff}\ D_o^{1/2}\ C\ v^{1/2}$$

where I_p, A_{eff}, C, $v^{1/2}$, $D_o^{1/2}$, and n indicate the effective surface area, solution concentration, the square root of scan rate, diffusion coefficient of phosphate, and electron number, respectively. The calculated effective surface area of the (Ga/CNT)@GCE was 5.24 cm^2 ($R^2 = 0.995$). Fig. 5c shows peak current (oxidation) vs scan rate (logI vs logV). The obtained slope was 0.3 for (Ga/CNT)@GCE ($R^2 = 0.990$).

The anodic peaks are attributed to the oxidation of CyS- at pH 7.0. Oxidation of CySH on an electrode can proceed through the following reaction [52,53];

$$CySH\ CyS^- + H^+ + e^- \quad (1)$$

The DPV study was conducted to determine the sensitivity of (Ga/CNT)@GCE for cysteine. The DPV curves for (Ga/CNT)@GCE at varying concentrations (0–1000 µM cysteine) in 0.1 M PBS and cysteine are depicted in Fig. 6. The DPV current densities vs cysteine exhibited a linear relationship within the range of 0–200 µM with current sensitivity of 0.0081 µA/µM (114 µA/mM cm^2) (Fig. 6b). This sensitivity value is

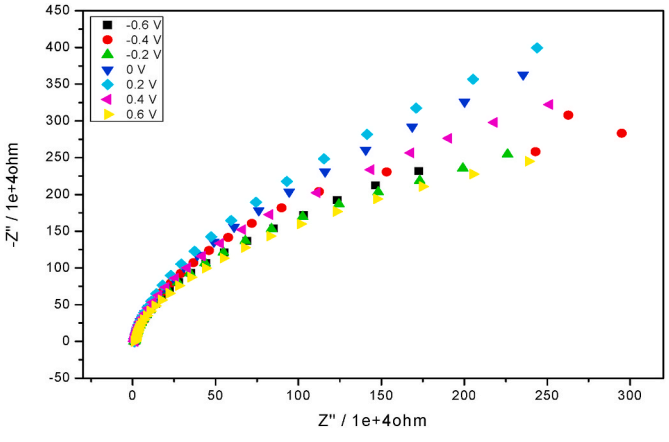

Fig. 7. Nyquist plots of (Ga/CNT)@GCE at different potentials in 0.1 M PBS (pH 7.2) + 5 mM cysteine solution.

greater than those reported in the literature. The LOD and limit of quantification were 0.05 and 0.15 µM at S/N = 3, respectively.

Fig. 7 shows the impedance behavior of (Ga/CNT)@GCE taken at

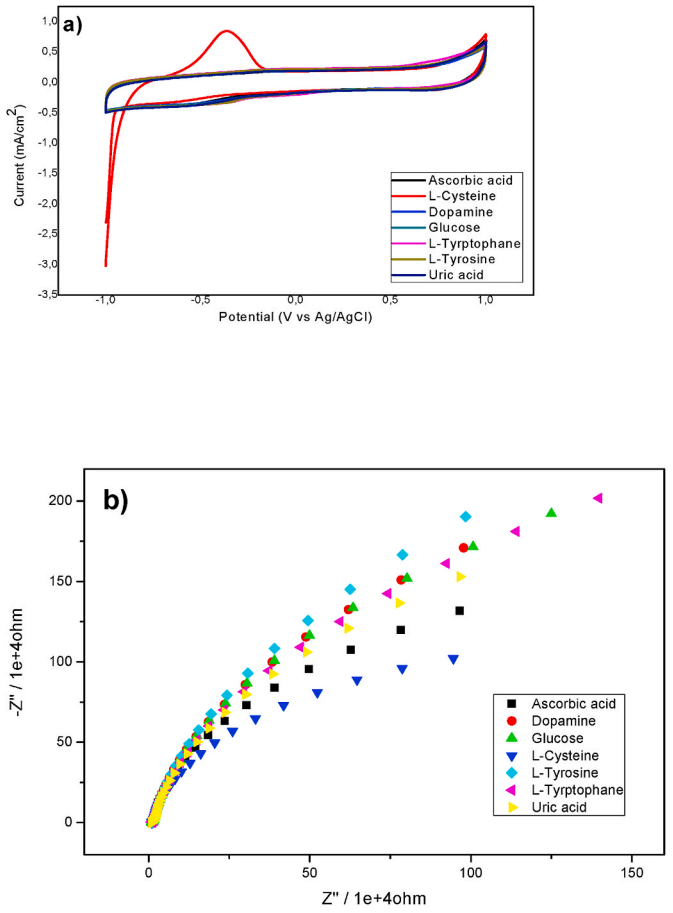

Fig. 8. (a) CV analysis (100 mV/s) and (b) EIS results (0.6 V) for interfering species of 0.1 mM uric acid, 0.1 mM ascorbic acid, 0.1 mM L-tryptophan, 0.1 mM L-tyrosine, 0.1 mM L-cysteine, and 0.1 mM dopamine on (Ga/CNT)@GCE.

varying potentials in PBS (0.1 M, pH 7.2) + cysteine (5 mM). The EIS results showed that cysteine electrooxidation on the GCE modified with Ga/CNT at various potentials had different electrochemical impedance behaviors. As mentioned above, the semicircular diameter of the impedance spectra is equal to the electron transfer resistance (R_{ct}); a large arc indicates that cysteine electrooxidation is slow but a small arc is indicative of fast electrooxidation kinetics. There was a clear decrease in arc diameter with increasing potential (Fig. 7), which can be interpreted as a decrease in R_{ct} of the cysteine electrooxidation reaction. The GCE modified with Ga/CNT had surface resistance at 0.6 V.

In experiments, the effects of some species mixed with other organics were investigated for cysteine determination based on blood samples. The selectivity measurements of the sensor were examined at 1 V potential with CV and EIS in the presence of ascorbic acid, D-glucose, uric acid, L-tyrosine, L-tryptophan, and dopamine, which are often found in biological fluids (Fig. 8a and b). The response for CV showed an increase in anodic peak current (Fig. 8a). Dopamine and L-tryptophan interference effects were greater than of uric acid, D-glucose, and L-tyrosine. Similarly, the EIS results were consistent in showing that L-cysteine had the lowest charge transfer (Fig. 8b). Thus, it is clear that the current and impedance responses of the noise were small enough to be ignored, indicating that the (Ga/CNT)@GCE had very good selectivity for cysteine detection.

For real sample measurements, the standard addition method was employed. For this measurement, a 600 mg acetylcysteine tablet was crushed to powder and homogenized. Then, 1 mg of acetylcysteine was placed into a 50-ml volumetric flask containing 0.1 M PBS solution at pH 7.0. Using this stock solution, 1.5 mM acetylcysteine was obtained by dilution and the sensor response was measured in this solution. Then 1.5 mM acetylcysteine was added to the actual sample solution and the sensor response was measured again. Recovery values were acceptable (Table 2). The relative standard deviation of the sample for six consecutive determinations was less than 3%. This result showed that the Ga/CNT-modified GCE performed well in the real sample.

Table 1
Electrode materials employed for electrochemical determination of cysteine. LOD, limit of detection.

Sensor	Sensitivity	Linear range	LOD	Reference
$CuFe_2O_4$/rGO-Au	100 μA/mM cm^2	0.05–0.2 μM	0.383 μM	[57]
AgNPs/GQDs/GCE	–	0.1–200 μM	1.1 μM	[58]
Ru(III) Schiff base complex	–	50–500 mg/L	0.11 mg/L	[59]
MoS_2/PDDA-MC	–	0.45–155 μM	0.09 μM	[60]

Table 2
Cysteine analysis data for acetyl cysteine drug sample.

Sample	Added (mM)	Found (mM)	Recovery (%)
1	1.5	1.52	98.7
2	3	3.1	96.7
3	6	5.8	96.7

4. Conclusions

In this study, the Ga/CNT catalyst was prepared by the chemical reduction method using $NaBH_4$. Characterization results from EDX-SEM and mapping analysis showed that the desired structure was successfully prepared. The H_2-TPR, O_2-TPO, and NH_3-TPD methods were used to characterize the surface chemical properties of the Ga/CNT catalyst. These results showed that the surface properties changed as a result of Ga addition. This could be explained by Ga/CNT having strong structure sensitivity. Electrochemical measurements (sensitivity determination, detection limit, interference study, and real sample analysis) were performed using (Ga/CNT)@GCE. Many previous studies have investigated the catalytic activity of Ga and showed an effect on increasing activity [54–56]. The (Ga/CNT)@GCE exhibited good electrocatalytic responses to cysteine with high sensitivity, stability, and selectivity. The Ga/CNT catalyst showed a linear response within the range of 0–200 μM with current sensitivity of 114 μA/mM cm^2 and a low detection limit of 0.05 μM. Several studies have examined electrochemical cysteine detection, and their sensitivity, linear range, and LOD values are summarized in Table 1. Comparison with the literature showed that (Ga/CNT)@GCE is a promising catalyst for simultaneous detection with high sensitivity at low concentrations. The (Ga/CNT)@GCE catalyst was unaffected by the presence of compounds commonly found in the body, such as D-glucose, uric acid, L-tyrosine, L-tryptophan, dopamine, and ascorbic acid. The (Ga/CNT)@GCE catalyst is a promising sensor for cysteine detection.

CRediT authorship contribution statement

Hilal Kivrak:Conceptualization, Methodology, Writing and Supervision, Writing – review & editing.Kadir Selçuk: Visualization, Investigation, Electrochemical measurements.Aykut Çağlar: Visualization, InvestigationNahit Aktas: Conceptualization, Methodology, Writing and Supervision.

Declaration of competing interest

The authors declare that they have no known competing financial interests or personal relationships that could have appeared to influence

the work reported in this paper.

Appendix A. Supplementary data

Supplementary data to this article can be found online at https://doi.org/10.1016/j.jpcs.2022.110836.

References

[1] E. Tanhaş, E. Martin, E.N. Korucu, T. Dirmenci, Effect of aqueous extract, hydrosol, and essential oil forms of some endemic *Origanum* L. (Lamiaceae) taxa on polyphenol oxidase activity in fresh-cut mushroom samples, J. Food Process. Preserv. 44 (2020), e14726.

[2] H. Takase, R.W. Regenhardt, Motor tract reorganization after acute central nervous system injury: a translational perspective, Neural Regen. Res. 16 (2021) 1144.

[3] S.K. Sinha, T.K. Upadhyay, S.K. Sharma, Nutritional-medicinal profile and quality categorization of fresh white button mushroom, Biointerface Res. Appl. Chem. 11 (2021) 8669–8685.

[4] C. Silva, M.C. Breitkreitz, M. Santhiago, C.C. Correa, L.T. Kubota, Construction of a new functional platform by grafting poly(4-vinylpyridine) in multi-walled carbon nanotubes for complexing copper ions aiming the amperometric detection of L-cysteine, Electrochim. Acta 71 (2012) 150–158.

[5] A.W. Ashor, M. Siervo, J.C. Mathers, Vitamin C, antioxidant status, and cardiovascular aging, in: Molecular Basis of Nutrition and Aging, Academic Press, 2016, pp. 609–619.

[6] B. Borek, T. Gajda, A. Golebiowski, R. Blaszczyk, Boronic acid-based arginase inhibitors in cancer immunotherapy, Bioorg, Med. Chem. 28 (2020), 115658.

[7] M. Bergagnini-Kolev, M. Howe, E. Burgess, P. Wright, S. Hamburger, Z. Zhong, S. B. Ellis, T.K. Ellis, Synthesis of trifluoromethyl substituted nucleophilic glycine equivalents and the investigation of their potential for the preparation of α-amino acids, Tetrahedron (2020), 131741.

[8] K. Kargosha, S. Ahmadi, M. Zeeb, S.R. Moeinossadat, Vapour phase Fourier transform infrared spectrometric determination of L-cysteine and L-cystine, Talanta 74 (2008) 753–759.

[9] C. Meese, D. Specht, D. Ratge, M. Eichelbaum, H. Wisser, High-performance liquid chromatographic and carbon-13 nuclear magnetic resonance spectrometric determination of S-carboxymethyl-L-cysteine and its metabolites in human urine, Fresenius' J. Anal. Chem. 346 (1993) 837–840.

[10] P. Rezanka, J. Koktan, H. Rezankova, P. Matejka, V. Kral, S, Spectrometric determination of L-cysteine and its enantiomeric purity using silver nanoparticles, Colloids Surf. A Physicochem. Eng. Asp. 436 (2013) 961–966.

[11] Z. Huang, Y. Yang, Y. Long, H. Zheng, A colorimetric method for cysteine determination based on the peroxidase-like activity of ficin, Anal. Methods 10 (2018) 2676–2680.

[12] L. Liu, G. Zhu, W. Zeng, Y. Yi, B. Lv, J. Qian, D. Zhang, Silicon quantum dot-coated onto gold nanoparticles as an optical probe for colorimetric and fluorometric determination of cysteine, Microchim. Acta 186 (2019) 1–9.

[13] N. Pan, W. Li-Ying, L.-L. Wu, C.-F. Peng, Z.-J. Xie, Colorimetric determination of cysteine by exploiting its inhibitory action on the peroxidase-like activity of Au@Pt core-shell nanohybrids, Microchim. Acta 184 (2017) 65–72.

[14] H. Rao, Y. Li, G. Zhang, Z. Xue, G. Zhao, S. Li, X. Du, A new colorimetric sensor for cysteine determination based on dual reacting-mediated strategy, Bull. Kor. Chem. Soc. 38 (2017) 1023–1027.

[15] S. Rastegarzadeh, F. Hashemi, Gold nanoparticles as a colorimetric probe for the determination of N-acetyl-L-cysteine in biological samples and pharmaceutical formulations, Anal. Methods 7 (2015) 1478–1483.

[16] H. Tavallali, G. Deilamy-Rad, N. Mosallanejad, Reactive Blue 4 as a single colorimetric chemosensor for sequential determination of multiple analytes with different optical responses in aqueous media: Cu^{2+}-cysteine using a metal ion displacement and Cu^{2+}-arginine through the host-guest interaction, Appl. Biochem. Biotechnol. 187 (2019) 913–937.

[17] J. Zhu, B.-Z. Zhao, Y. Qi, J.-J. Li, X. Li, J.-W. Zhao, Colorimetric determination of Hg (II) by combining the etching and aggregation effect of cysteine-modified Au-Ag core-shell nanorods, Sensor. Actuator. B Chem. 255 (2018) 2927–2935.

[18] Z. Zheng, Q. Feng, J. Li, C. Wang, The p-type MoS_2 nanocube modified poly (diallyl dimethyl ammonium chloride)-mesoporous carbon composites as a catalytic amplification platform for electrochemical detection of L-cysteine, Sensor. Actuator. B Chem. 221 (2015) 1162–1169.

[19] J. Yao, C. Liu, L. Liu, M. Chen, M. Yang, An electrochemical sensor for sensitive determination of L-cysteine and its electrochemical kinetics on AgNPs/GQDs/GCE composite modified electrode, J. Electrochem. Soc. 165 (2018) B551.

[20] C. Xiao, J. Chen, B. Liu, X. Chu, L. Wu, S. Yao, Sensitive and selective electrochemical sensing of l-cysteine based on a caterpillar-like manganese dioxide–carbon nanocomposite, Phys. Chem. Chem. Phys. 13 (2011) 1568–1574.

[21] M. Pazalja, E. Kahrović, A. Zahirović, E. Turkušić, Electrochemical sensor for determination of L-cysteine based on carbon electrodes modified with Ru (III) Schiff base complex, carbon nanotubes and Nafion, Int. J. Electrochem. Sci. 11 (2016) 10939–10952.

[22] S. Nyoni, T. Mugadza, T. Nyokong, Improved L-cysteine electrocatalysis through a sequential drop dry technique using multi-walled carbon nanotubes and cobalt tetraaminophthalocyanine conjugates, Electrochim. Acta 128 (2014) 32–40.

[23] A. Kurniawan, F. Kurniawan, F. Gunawan, S.-H. Chou, M.-J. Wang, Disposable electrochemical sensor based on copper-electrodeposited screen-printed gold electrode and its application in sensing L-cysteine, Electrochim. Acta 293 (2019) 318–327.

[24] M. Heidari, A. Ghaffarinejad, Electrochemical sensor for L-cysteine by using a cobalt (II)/aluminum (III) layered double hydroxide as a nanocatalyst, Electrochim. Acta 186 (2019) 365.

[25] M. Ahmad, C. Pan, J. Zhu, Electrochemical determination of L-cysteine by an elbow shaped, Sb-doped ZnO nanowire-modified electrode, J. Mater. Chem. 20 (2010) 7169–7174.

[26] A. Caglar, H.Ç. Kazıcı, D. Alpaslan, Y. Yılmaz, H. Kivrak, N. Aktas, 3-Acrylamidopropyl-trimethylammoniumchloride cationic hydrogel modified graphite electrode and its superior sensitivity to hydrogen peroxide, Fullerenes, Nanotub. Carbon Nanostruct. 27 (2019) 736–745.

[27] N.A. Ertas, E. Kavak, F. Salman, H.C. Kazici, H. Kivrak, A. Kivrak, Synthesis of ferrocene based naphthoquinones and its application as novel non-enzymatic hydrogen peroxide, Electroanalysis 32 (2020) 1178–1185.

[28] H.C. Kazici, F. Salman, H.D. Kivrak, Synthesis of Pd–Ni/C bimetallic materials and their application in non-enzymatic hydrogen peroxide detection, Mater. Sci. Poland 35 (2017) 660–666.

[29] H.Ç. Kazıcı, M. Yayla, B. Ulaş, N. Aktaş, H. Kivrak, Development of nonenzymatic benzoic acid detection on PdSn/GCE/Vulcan XC-72R prepared via polyol method, Electroanalysis 31 (2019) 1118–1124.

[30] H. Kivrak, O. Alal, D. Atbas, Efficient and rapid microwave-assisted route to synthesize Pt–MnOx hydrogen peroxide sensor, Electrochim. Acta 176 (2015) 497–503.

[31] R. Majidi, A.R. Karami, K. Rahmani, A.M. Khairogli, Electronic properties of hydrogenated porous graphene based nanoribbons: a density functional theory study, Int. J. Nano Dimens. (IJND) 11 (2020) 112–119.

[32] O. Sahin, H. Kivrak, A. Kivrak, H.Ç. Kazıcı, O. Alal, D. Atbas, Facile and rapid synthesis of microwave assisted Pd nanoparticles as non-enzymatic hydrogen peroxide sensor, Int. J. Electrochem. Sci. 12 (2017) 762–769.

[33] F. Salman, H.C. Kazici, H. Kivrak, Engineering, Electrochemical sensor investigation of carbon-supported PdCoAg multimetal catalysts using sugar-containing beverages, Front. Chem. Sci. Eng. 14 (2019) 1–10.

[34] C. Beasley, M.K. Gnanamani, H.H. Hamdeh, M. Martinelli, B.H. Davis, Effect of gallium additions on reduction, carburization and Fischer–Tropsch activity of iron catalysts, Catal. Lett. 148 (2018) 1920–1928.

[35] U. Mehmood, W. Ahmad, S. Ahmed, Nickel impregnated multi-walled carbon nanotubes (Ni/MWCNT) as active catalyst materials for efficient and platinum-free dye-sensitized solar cells (DSSCs), Sustain, Energy Fuels 3 (2019) 3473–3480.

[36] Y. Feng, G. Zhou, G. Wang, M. Qu, Z. Yu, Removal of some impurities from carbon nanotubes, Chem. Phys. Lett. 375 (2003) 645–648.

[37] J. Van Doorn, M.A. Vuurman, P. Tromp, D. Stufkens, J. Moulijn, Correlation between Raman spectroscopic data and the temperature-programmed oxidation reactivity of coals and carbons, Fuel Process. Technol. 24 (1990) 407–413.

[38] P.J. Barrie, Analysis of temperature programmed desorption (TPD) data for the characterisation of catalysts containing a distribution of adsorption sites, Phys. Chem. Chem. Phys. 10 (2008) 1688–1696.

[39] V. Rakić, L. Damjanović, Temperature-programmed desorption (TPD) methods, in: Calorimetry and Thermal Methods in Catalysis, Springer, 2013, pp. 131–174.

[40] C.-T. Shao, W.-Z. Lang, X. Yan, Y.-J. Guo, Catalytic performance of gallium oxide based-catalysts for the propane dehydrogenation reaction: effects of support and loading amount, RSC Adv. 7 (2017) 4710–4723.

[41] M. Ahmad, C.F. Pan, J. Zhu, Electrochemical determination of L-cysteine by an elbow shaped, Sb-doped ZnO nanowire-modified electrode, J. Mater. Chem. 20 (2010) 7169–7174.

[42] C.H. Xiao, J.H. Chen, B. Liu, X.C. Chu, L.A. Wu, S.Z. Yao, Sensitive and selective electrochemical sensing of L-cysteine based on a caterpillar-like manganese dioxide-carbon nanocomposite, Phys. Chem. Chem. Phys. 13 (2011) 1568–1574.

[43] S. Nyoni, T. Mugadza, T. Nyokong, Improved L-cysteine electrocatalysis through a sequential drop dry technique using multi-walled carbon nanotubes and cobalt tetraaminophthalocyanine conjugates, Electrochim. Acta 128 (2014) 32–40.

[44] Z.X. Zheng, Q.L. Feng, J. Li, C.M. Wang, The p-type MoS_2 nanocube modified poly (diallyl dimethyl ammonium chloride)-mesoporous carbon composites as a catalytic amplification platform for electrochemical detection of L-cysteine, Sensor. Actuator. B Chem. 221 (2015) 1162–1169.

[45] M. Pazalja, E. Kahrovic, A. Zahirovic, E. Turkusic, Electrochemical sensor for determination of L-cysteine based on carbon electrodes modified with Ru(III) Schiff base complex, carbon nanotubes and Nafion, Int. J. Electrochem. Sci. 11 (2016) 10939–10952.

[46] J. Yao, C.H. Liu, L. Liu, M. Chen, M. Yang, An electrochemical sensor for sensitive determination of L-cysteine and its electrochemical kinetics on AgNPs/GQDs/GCE composite modified electrode, J. Electrochem. Soc. 165 (2018). B551–B558.

[47] M. Heidari, A. Ghaffarinejad, Electrochemical sensor for L-cysteine by using a cobalt(II)/aluminum(III) layered double hydroxide as a nanocatalyst, Microchim. Acta 186 (2019) 365.

[48] A. Kurniawan, F. Kurniawan, F. Gunawan, S.H. Chou, M.J. Wang, Disposable electrochemical sensor based on copper-electrodeposited screen-printed gold electrode and its application in sensing L-cysteine, Electrochim. Acta 293 (2019) 318–327.

[49] D. Zhu, Q. Zhen, J. Xin, H. Ma, L. Tan, H. Pang, X. Wang, A free-standing and flexible phosphorus/nitrogen dual-doped three-dimensional reticular porous carbon frameworks encapsulated cobalt phosphide with superior performance for nitrite detection in drinking water and sausage samples, Sensor. Actuator. B Chem. 321 (2020), 128541.

[50] D. Zhu, H. Ma, Q. Zhen, J. Xin, L. Tan, C. Zhang, X. Wang, B. Xiao, Hierarchical flower-like zinc oxide nanosheets in-situ growth on three-dimensional ferrocene-

functionalized graphene framework for sensitive determination of epinephrine and its oxidation derivative, Appl. Surf. Sci. 526 (2020), 146721.
[51] D. Zhu, Z. Bai, H. Ma, L. Tan, H. Pang, X. Wang, High performance simultaneous detection of β-nicotinamide adenine dinucleotide and l-tryptophan in human serum based on a novel nanocomposite of ferroferric oxide-functionalized polyoxometalates, Sensor. Actuator. B Chem. 309 (2020), 127787.
[52] M. Pazalja, E. Kahrović, A. Zahirović, E. Turkušić, Electrochemical sensor for determination of L-cysteine based on carbon electrodes modified with Ru (III) Schiff base complex, carbon nanotubes and Nafion, Int. J. Electrochem. Sci. 11 (2016) 10939–10952.
[53] Z. Chen, H. Zheng, C. Lu, Y. Zu, Oxidation of L-cysteine at a fluorosurfactant-modified gold electrode: lower overpotential and higher selectivity, Langmuir 23 (2007) 10816–10822.
[54] E. Puello-Polo, Y. Pájaro, E. Márquez, Effect of the gallium and vanadium on the dibenzothiophene hydrodesulfurization and naphthalene hydrogenation activities using sulfided nimo-V_2O_5/Al_2O_3-Ga_2O_3, Catalysts 10 (2020) 894.
[55] B. Ulas, D. Alpaslan, Y. Yilmaz, T.E. Dudu, O.F. Er, H. Kivrak, Disentangling the enhanced catalytic activity on Ga modified Ru surfaces for sodium borohydride electrooxidation, Surface. Interfac. 23 (2021), 100999.
[56] E. Lalik, X. Liu, J. Klinowski, Role of gallium in the catalytic activity of zeolite [Si, Ga]-ZSM-5 for methanol conversion, J. Phys. Chem. 96 (1992) 805–809.
[57] K. Atacan, $CuFe_2O_4$/reduced graphene oxide nanocomposite decorated with gold nanoparticles as a new electrochemical sensor material for L-cysteine detection, J. Alloys Compd. 791 (2019) 391–401.
[58] J. Yao, C. Liu, L. Liu, M. Chen, M. Yang, An electrochemical sensor for sensitive determination of L-cysteine and its electrochemical kinetics on AgNPs/GQDs/GCE composite modified electrode, J. Electrochem. Soc. 165 (2018). B551–B558.
[59] M. Pazalja, E. Kahrovic, A. Zahirovic, E. Turkusic, Electrochemical sensor for determination of L-cysteine based on carbon electrodes modified with Ru(III) Schiff base complex, carbon nanotubes and Nafion, Int. J. Electrochem. Sci. 2016 (2016), 10939, 10952.
[60] Z.-X. Zheng, Q. Feng, J. Li, C.-M. Wang, The p-type MoS_2 nanocube modified poly (diallyl dimethyl ammonium chloride)-mesoporous carbon composites as a catalytic amplification platform for electrochemical detection of L-cysteine, Sensor. Actuator. B Chem. 221 (2015).